

# Correlation Between Surface Morphology Evolution and Grain Structure: Whisker/Hillock Formation in Sn-Cu

FEI PEI,<sup>1,2</sup> NITIN JADHAV,<sup>1</sup> and ERIC CHASON<sup>1</sup>

1.—School of Engineering, Brown University, Providence, RI 02912, USA. 2.—e-mail: fei\_pei@brown.edu

Sn whisker and hillock formation is a reliability risk that has become increasingly important as the electronics industry has moved toward Pb-free manufacturing. To prevent them, we would like to understand what makes specific sites susceptible to deform into whiskers. We have used *in situ* scanning electron microscopy (SEM)/electron backscattering diffraction (EBSD) to monitor simultaneously the evolution of surface morphology and grain orientation in Sn surfaces in order to correlate whisker/hillock initiation with the underlying microstructure. Because rough films are difficult to measure with EBSD, we developed a unique procedure to make Sn-Cu samples with ultra-flat surfaces so that a large fraction of Sn grains can be indexed over repeated scans. We find that whiskers/hillocks grow from existing grains (not re-nucleated grains) with orientations close to (001). They often rotate from the as-deposited structure so that the orientation after growth does not indicate the orientation from which the whisker initiated. We measured the interface structure after removal of the Sn layer by chemical etching and found that there is no excessive accumulation of intermetallic compound around the whisker/hillock roots. Cross-sectional measurements revealed that a large fraction of the whiskers/hillocks have oblique boundaries underneath the surface, supporting the idea that these allow whiskers/hillocks to grow with lower stress.

## INTRODUCTION

The co-evolution of surface morphology and microstructure is important in many thin film systems; e.g., grain growth, interfacial reactions, pitting, etc. can all affect the film's properties and performance. In this work, we focus on Sn whiskers, i.e., needle-like features that grow spontaneously out of Sn coatings on Cu and can cause short circuits. Our goal is to understand why whiskers grow out of specific sites on the surface. Are these sites present in the as-deposited film or do they nucleate later? Is it their orientation or something else about the structure that makes them susceptible to deformation?

Electron backscattering diffraction (EBSD) is a useful tool for studying grain orientation, but it cannot be used on the typically rough surfaces found in electroplated Sn samples. Therefore, we have developed a special method to produce flat surfaces that can be monitored repeatedly in real time. Using

these flat samples, we can simultaneously measure the surface and grain structure as it evolves in real time. We also can correlate the surface evolution with intermetallic compound (IMC) formation at the Sn-Cu interface by chemically stripping the Sn layer and aligning the sample to look at the same region.

The risk of Sn whiskers in electronics systems has been recognized since the early 1950s, and these conducting filaments have been reported to cause many system failures.<sup>1</sup> Adding Pb to Sn was found to suppress whisker formation,<sup>2</sup> which was the accepted mitigation method for four decades. However, legislation restricting the use of hazardous substances for environmental reasons has promoted a transition to Pb-free manufacturing, which makes whiskers a reemerging problem. Although other alloying metals [Ag, Ni, Au, and Bi]<sup>3–6</sup> and film structures<sup>7</sup> have been considered or adopted by electronic manufacturers, none of these methods

prevents whiskering as efficiently as Pb addition. The difficulty of finding a replacement for Pb highlights the need for understanding the basic mechanisms underlying their growth to guide the formation of better mitigation strategies.

Previous studies provide us with a general picture of why whiskers (and other lower aspect ratio features called hillocks) grow out of Sn-Cu samples. The primary driving force for whiskering is believed to come from the compressive stress introduced into the Sn layer by continuous formation of IMCs at the Sn-Cu interface.<sup>8-12</sup> The whiskers/hillocks grow out of the surface in response to this stress, although whiskering is not the only (or necessarily primary) way for stress to relax.<sup>13</sup> Dislocation motion, stress-driven diffusion, and power-law creep<sup>14</sup> also relax stress, although the tenacious oxide on top of the Sn film prevents rapid relaxation by diffusion or dislocation motion to the surface.<sup>15</sup>

Perhaps the most important outstanding question with respect to whisker growth is why certain sites on Sn surfaces grow into whiskers/hillocks but others do not. Understanding this would allow us to focus mitigation efforts on reducing the number of susceptible sites in the film. In fact, only a very small fraction of grains (typically 1 out of  $10^3$ – $10^4$ ) become whiskers or hillocks, and it is not known what makes them susceptible to deformation. Real-time scanning electron microscopy (SEM) studies of growth<sup>16</sup> show that the grains that initiate whisker/hillock growth are initially indistinguishable from their neighbors. No apparent defect or impurity was found that indicated these grains were different from the rest. A weakness in the oxide might also tend to promote whisker/hillock growth because they need to penetrate the oxide in order to pop out. However, removal of the oxide in selected regions by a focused ion beam (FIB) did not induce whiskers/hillocks to grow out of these modified sites.<sup>16</sup> Weakening the oxide is therefore not sufficient to induce whiskering.

These results indicate that the underlying microstructure of the layer must play a critical role in determining whether whiskering will occur. Finite element analysis (FEA) modeling has shown that a whisker-like feature can develop from a “weak” grain that has lower stress than its neighbors when the film is uniformly strained.<sup>13</sup> As Sn has highly anisotropic mechanical properties, the magnitude of the stress or the stress required for yielding may differ among grains with different orientations in a typical polycrystalline Sn film. Alternatively, the structure underneath a grain may affect the stress needed to make it deform; the presence of horizontal grain boundaries<sup>10,17</sup> at the root of a whisker/hillock has been suggested as a means for addition of atoms to the grain with less stress than in columnar grains. If such “weak” grains are not present in the film, new grains may be created by dynamic recrystallization<sup>18</sup> that can form into whiskers/hillocks. The formation of IMCs

at the Cu-Sn interface may also influence the tendency of the Sn grain to deform.

To differentiate among these various potential mechanisms, we have performed measurements to correlate the evolution of surface morphology with the Sn layer’s microstructure. We use SEM and EBSD to measure repeatedly the surface morphology and orientation of the grains in the Sn film, both before and after whiskers/hillocks form.

Surface roughness can limit the efficiency of EBSD on samples such as traditional Sn electro-deposited layers.<sup>19</sup> Chemical mechanical polishing is often recommended to smooth the surface before EBSD measurements. However, polished Sn samples are observed to have quite different whiskering behavior from unpolished ones, including the length of dormancy and whisker density.<sup>20</sup> We have therefore developed a novel method (“peel-off”) that enables us to prepare samples with ultra-flat surfaces without introducing impurities and plastic deformation that are likely to occur in the process of polishing. The “peel-off” method, described in detail below, is a general technique that can be used to create flat surfaces for EBSD characterization in other systems as well. The smooth morphology enables a high fraction of grains to be indexed on these samples by EBSD with mean angular deviation (MAD) smaller than  $1^\circ$ . Such efficiency can be maintained when similar scans are repeated in the same region, which allows us to monitor surface morphology and grain structure simultaneously in real time.

### Preparing Samples with Flat Surface Using “Peel-Off” Method

As shown schematically in Fig. 1, the peel-off method consists of two consecutive steps, deposition and peeling. In the deposition step (Fig. 1a), a Sn film is deposited onto a cleaned glass substrate by electron-beam evaporation with a base pressure of  $3 \times 10^{-6}$  torr. Cu is then evaporated over the Sn layer. As the glass substrate is flat, the Sn interface with the glass is also flat. After removal from the vacuum chamber, the fresh bi-layer sample is attached to a silicon base by carbon tape, as shown in Fig. 1b. As the adhesion between the Sn film and the glass is weak, the substrate can then be “peeled off” without damage to expose the smooth side of Sn for EBSD characterization. An SEM image of a peel-off sample with  $1.5\text{-}\mu\text{m}$  Sn on  $0.5\text{-}\mu\text{m}$  Cu (Fig. 1c) shows the resulting smooth surface and the shape of individual grains. This sample surface was measured within an hour after deposition. An FIB cross section (Fig. 1d) shows that the microstructure of another peel-off sample ( $1\text{-}\mu\text{m}$  Sn on  $0.6\text{-}\mu\text{m}$  Cu) is polycrystalline with a columnar structure, similar to the structure of electroplated Sn films. The surface of the Sn layer, which was peeled from the glass, is significantly smoother than the Sn-Cu interface because the layer becomes rougher as it grows.

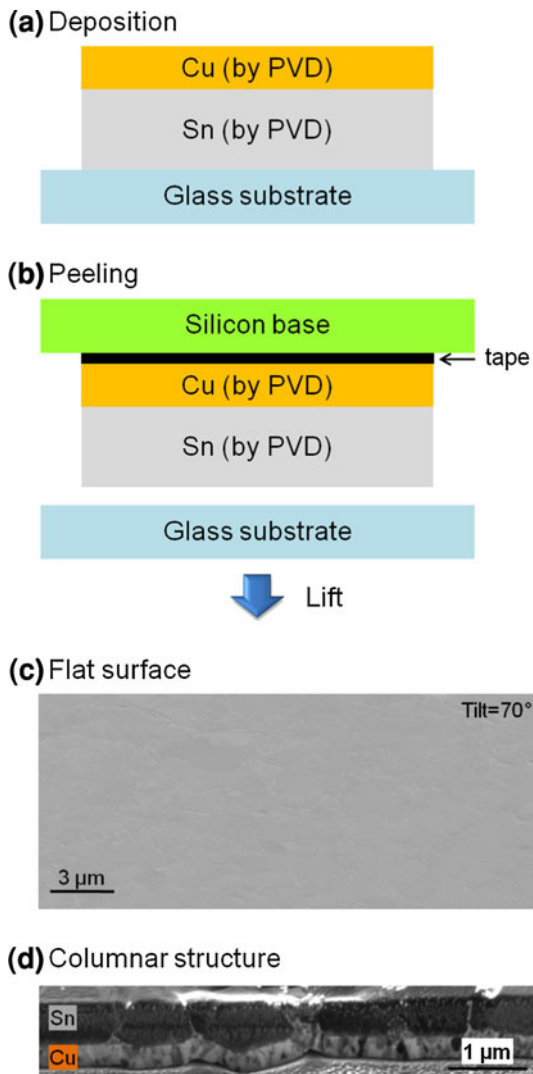


Fig. 1. Sketches of (a) deposition and (b) peeling steps in the peel-off preparation method. The smooth surface and the columnar structure of the peel-off samples are shown in (c) and (d).

### ***In Situ* SEM/EBSD Measurements of Surface Morphology and Grain Orientation**

We performed real-time SEM/EBSD measurements to correlate whisker/hillock growth with the grain orientation and microstructural evolution. Results from a “peel-off” sample with 1.6- $\mu\text{m}$  Sn/0.6- $\mu\text{m}$  Cu are shown in Fig. 2; a 60- $\mu\text{m}$   $\times$  45- $\mu\text{m}$  region was monitored repeatedly over a period of 65 h. The sample was transferred into the SEM/EBSD system within an hour after deposition, and it was kept in vacuum during the subsequent EBSD measurements. The images show the surface morphology (Fig. 2a, c, e) and crystal orientation map (Fig. 2b, d, f) from three consecutive scans started at 1, 5, and 9 h after deposition. The SEM images show the surface morphology right before each EBSD scan was started. The SEM image in Fig. 2a indicates that the area of interest was flat and initially whisker-free.

The normal direction crystal orientation maps in Fig. 2b, d, and f were plotted by using Tango software (developed by the Oxford Instruments Company, Oxfordshire, U.K.). The color in the orientation maps corresponds to the orientation of the planes parallel to the sample surface. The schematic shown in the panel below Fig. 2f indicates how the color of each point is related to the crystal orientation in the stereographic triangle. Sn is a tetragonal system so that the (100) and (010) planes have equal spacing while the (001) planes are different. The points that were not indexed in the scan are colored as black in the orientation map. In some regions, where adjacent grains have similar crystal orientations, color contrast alone is not enough to indicate grain shape so that the grain boundaries with boundary angles larger than  $5^\circ$  are also highlighted by black lines in the orientation maps. The normal direction inverse pole figure (IPF) from Fig. 2b is also shown below Fig. 2f. The contour coloring is chosen so that the darker color indicates a larger fraction of grains having that orientation. The as-deposited samples have a bimodal texture with the majority of grains having (010) or (001) type orientation, colored as green and red in the orientation map, respectively. There were only a small number of grains with other orientations, i.e., yellow, blue, or purple grains that can be seen in Fig. 2b; their fraction was too small to be indicated on the inverse pole figure. Note that samples grown by other methods or on other substrates may have different textures than the peel-off samples discussed here.<sup>21–23</sup>

From the SEM image in Fig. 2c, four hillocks were observed to have grown out of the measured region at 5 h after deposition. The circles drawn on the orientation map (Fig. 2b) are centered at the same places where the hillocks form in Fig. 2c. We found that hillocks typically grew from configurations that have red grains (with (001)-type orientation) surrounded by green ones (with (010)-type orientation).<sup>24</sup> After the hillocks start to grow out, a large rotation of the surface makes it so these hillock grains can no longer be measured by the EBSD. The electron beam also gets scattered by the hillocks before it can reach the neighboring grains to produce kikuchi patterns necessary for indexing, resulting in the black areas surrounding the hillocks in the orientation map (Fig. 2d). In the regions away from the hillocks, however, we find the grain structure is essentially unchanged from the as-deposited grain structure.

At 9 h after deposition, three of the four hillocks continued to grow, as seen in the SEM image in Fig. 2e. Consequently, the black regions around these growing hillocks also became larger in the EBSD mapping on this surface. In the areas that still could be indexed, no large-scale grain growth was observed during whisker/hillock growth. Similar behavior is also seen in experiments on other peel-off samples that have been monitored over a period of 2 days.

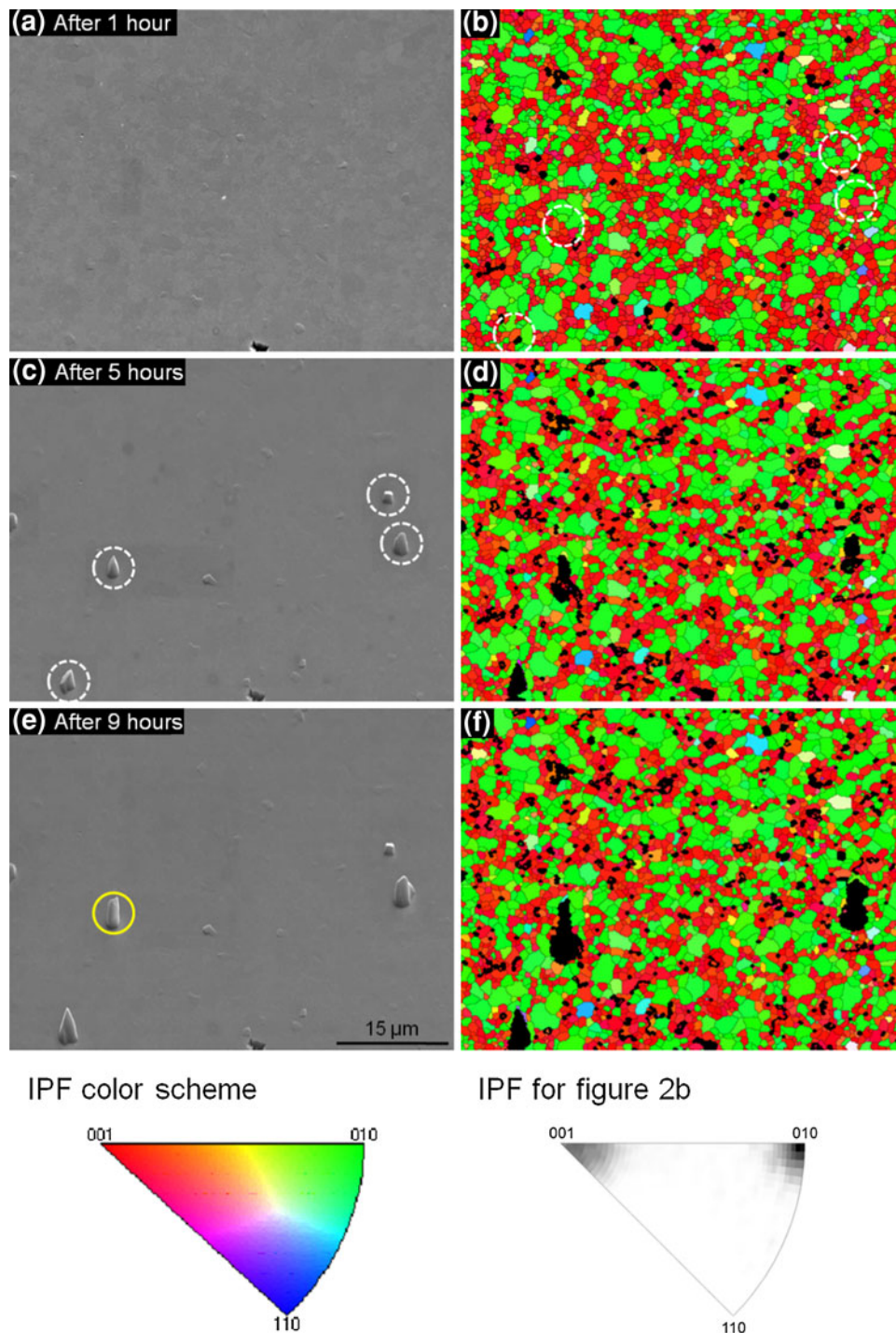


Fig. 2. SEM images (a, c, e) and crystal orientation maps (b, d, f) measured at 1 h, 5 h, and 9 h after deposition. The inverse pole figure shows the color key used for the points in the orientation maps.

After the three EBSD measurements, the sample was taken out of the chamber and stored in ambient. At about 40 h after deposition, the surface and morphology for the selected region was reexamined by putting the sample back to the SEM/EBSD system and measuring the same region. At that time, two new hillocks were found to have emerged from the site close to the hillock that is indicated by a

yellow circle in Fig. 2e. A set of SEM images showing their evolution is given in Fig. 3. The grains that formed into the hillocks were originally level with the rest of the surface (Fig. 3a), and there is no indication that these grains will start to form whiskers/hillocks. The hillock initiation (after 40 h, Fig. 3b) starts with cracking of the oxide and lifting up of the grain around its grain boundaries. The fact

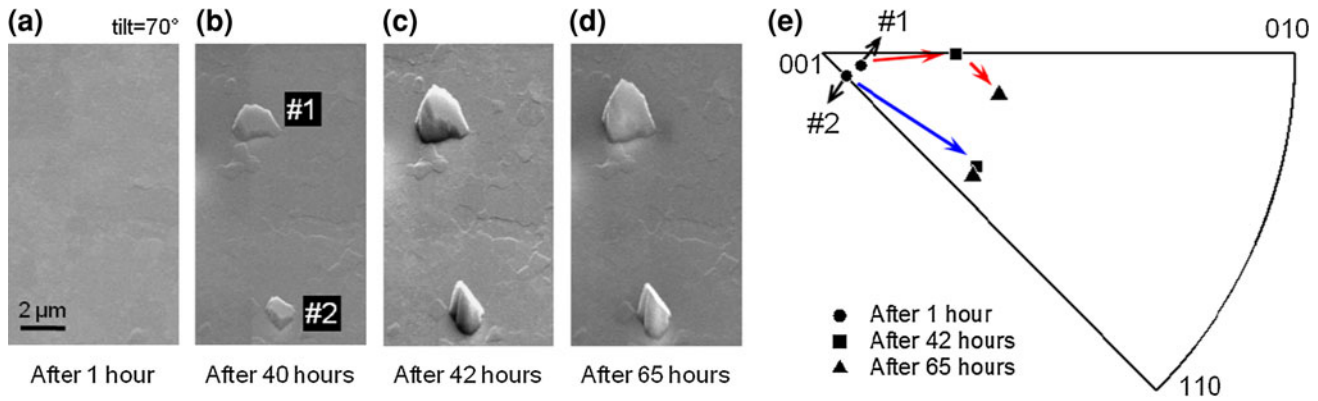


Fig. 3. SEM images of Sn surface after (a) 1 h, (b) 40 h, (c) 42 h, and (d) 65 h. (e) Hillock orientations acquired at different times.

that the shape of the hillocks is the same as the grains before they started to grow shows that they come from Sn grains that were present after deposition rather than from new grains created in the dormancy period. This tendency to form from pre-existing grains was found repeatedly<sup>24</sup> and suggests that recrystallization is not required for hillocks to form on this sample (although it may be possible in other cases).

As these hillocks grew, we were able to monitor the evolution of their grain orientation and to find that they rotate substantially. The initial orientations of the grains before the hillocks form are indicated by the solid circles in the inverse pole figure shown in Fig. 3e. Like the other hillocks, these hillocks develop from red grains with orientations close to (001). Rotation of the top surface of the hillock can be seen in the SEM images; other real-time studies of hillock growth<sup>16</sup> also show a significant amount of surface rotation. However, in this case, we were able to use EBSD to measure their orientation change over time since the deformation was small. The orientations measured after 42 h and after 65 h are indicated by the solid squares and solid triangles in Fig. 3e. It is clear that the grain orientations of the two hillocks change significantly from their respective as-deposited orientations. Moreover, although the two hillocks start from grains with similar orientations, their orientation after growth is very different in each case. These results provide an important warning regarding measurements of whiskers or hillocks: The orientations measured after whiskers/hillocks have formed may not be indicative of what their orientations were initially. For this reason, we believe it is necessary to conduct measurements before and after they form to determine which orientations have the greatest propensity to form whiskers/hillocks.

### Distribution of IMC Particles at the Sn-Cu Interface

Although we see a tendency for hillocks to grow from grains with (001)-type orientation surrounded by (010) grains, it is also noted that many similar

grain configurations did not form into whiskers/hillocks. Therefore, the grain structure is one but not the only decisive factor for determining where whiskers/hillocks form in these peel-off samples.

One factor that may also play a role is the distribution of IMC particles at the Sn-Cu interface. To characterize the sub-surface IMC, we made SEM images after selectively etching away the Sn to reveal the IMC below of the same regions that we had characterized with SEM/EBSD. To allow the images before and after stripping to be overlaid, we created fiducial marks on the sample that enabled us to reposition the sample precisely after remounting in the microscope. The error in placement from the initial position was within several microns. In this way, we could determine how the IMC is distributed around the hillock roots and under the regions free of whiskers/hillocks as well. This method also enables us to observe a much larger surface area than cross-sectional images.

The correlation among grain structure, surface morphology, and IMC growth is shown in Fig. 4. The EBSD-determined grain structure of a selected region made 1 h after deposition is shown in Fig. 4a. The corresponding surface morphology at 331 h after deposition (Fig. 4b) indicates the presence of three hillocks. Circles are drawn on both images to relate the position of the hillocks to the crystal orientation map. The Sn is then removed by selective chemical etching that does not affect the IMC at the Sn-Cu interface. An SEM image of the IMC structure exposed after stripping from the identical region is shown in Fig. 4c. The grain boundaries from the EBSD scan are superimposed on top of the IMC image as red lines. As the Sn film has a columnar microstructure, the grain structure measured by EBSD at the surface is expected to be similar to the grain structure at the Cu-Sn interface. This allows us to observe that the configuration of IMC particles aligns with the grain structure at many sites. This is consistent with previous studies that suggested that IMC particles nucleate preferentially around grain boundaries at the interface.<sup>25</sup>

The positions of the hillocks relative to the IMC are shown by the circles in Fig. 4c. This measurement lets us directly study the IMC at the root of the hillock after the Sn is stripped. We find that there is no more IMC along the boundaries of the hillock grains than the other grains, implying no excess IMC particle formation is required to drive formation of the surface features from these sites. Similarly, no whiskers/hillocks were seen to develop over other zones where very large IMC particles were observed. This suggests that formation of whiskers/hillocks does not directly correlate with IMC growth. This observation is consistent with the results from our FEA simulation,<sup>26</sup> which show that the compressive stress is initially localized around the IMC particles, but grain boundary diffusion, which is very active in Sn, together with plasticity, helps to spread out the stress so that its distribution through the Sn film eventually becomes relatively uniform.

### Oblique Grain Boundaries

The results discussed above rule out surface defects, a weak oxide, dynamic recrystallization, or excessive IMC growth as the dominant reasons for whiskers/hillocks to nucleate at particular surface sites. We therefore studied the microstructure under the whisker/hillock to determine whether horizontal/oblique grain boundaries (or V-grooves) are present that allow the grains to be sinks for diffusing atoms.<sup>17</sup> As the EBSD technique is only sensitive to grains at the surface of the film, we used the FIB to make cross sections of the hillocks to examine the sub-surface structures. An image from a peel-off sample (Fig. 5a, 1.5- $\mu\text{m}$  Sn on 0.6- $\mu\text{m}$  Cu), taken at 183 h after deposition shows 11 hillocks over an area of 60  $\mu\text{m}$   $\times$  60  $\mu\text{m}$ . We made cross-sectional measurements of nine hillocks (dashed lines are drawn in Fig. 5a to show the

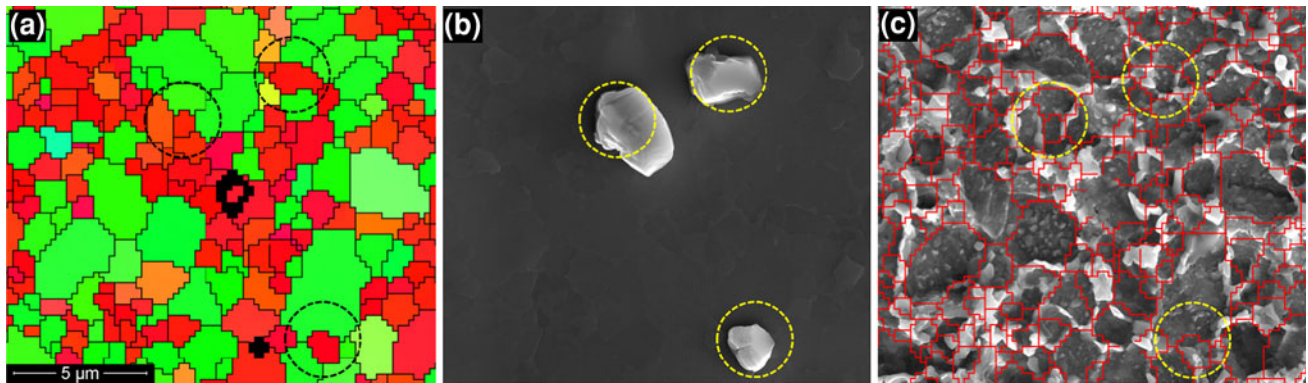


Fig. 4. (a) Grain structure measured 1 h after deposition, (b) surface morphology measured 331 h after deposition, and (c) IMC structure at the interface after stripping of Sn layer. The grain boundaries from (a) are superimposed over the IMC image. The dashed circles indicate the positions of the hillocks.

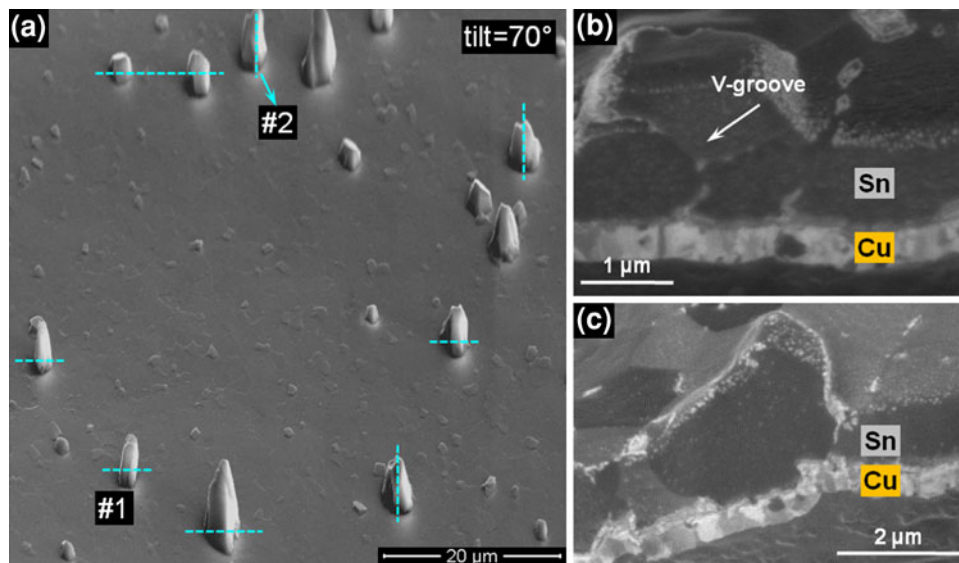


Fig. 5. (a) SEM image of surface morphology at 183 h after deposition. Dashed lines are drawn to show the direction of cross sections. (b) Cross-sectional image of hillock #1 in (a). (c) Cross-sectional image of hillock #2.

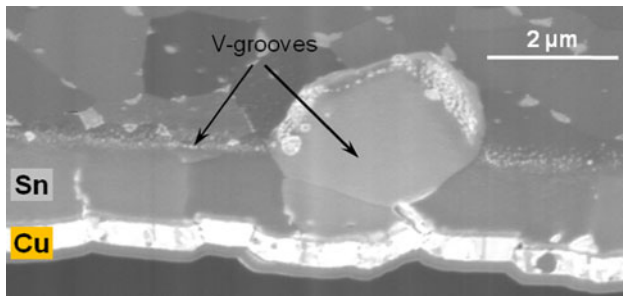


Fig. 6. Cross-sectional image showing v-groove under a hillock and another v-groove with no hillock.

direction of the cross sections) and found that six have horizontal/oblique grain boundaries under them. An example is given in Fig. 5b, with the arrow showing the presence of the V-groove (oblique boundary). Two samples were found to have the grain of the hillock extending through the entire thickness of the Sn layer, such as the one in Fig. 5c. But in most cases, the whiskers/hillocks have horizontal or oblique boundaries under the surface, pointing to the influences of the sub-surface structure on whisker-forming propensity.

Such horizontal boundaries might be present in the as-deposited film or they could form later, through nucleation of surface grains or sub-grain boundary formation (due to accumulation of dislocations produced by the expanding IMC particles<sup>27</sup>). The EBSD and SEM results studies discussed above suggest that, at least for the sample system discussed here, the grains that form hillocks are already present in the first measurements of the sample (at 1 h after deposition). As further evidence, in one cross-sectional image (Fig. 6), we found a hillock that had a v-groove under the surface, and the grain next to it had a v-groove as well that had not turned into a whisker/hillock yet. A hillock feature might have initiated from this grain later if we had not cross-sectioned it, or perhaps it needed larger stress to be activated. Cross sections of some pure Sn peel-off samples without Cu layers also had V-grooves, which indicates that IMC formation or stress relaxation are not necessary for them to form. It is possible that the peel-off technique for making samples might have a larger tendency to produce v-grooves and surface grains than for typical electroplated samples. This remains to be studied.

### SUMMARY

In summary, we have used real-time SEM/EBSD measurements to track simultaneously the evolution of microstructure and surface morphology on Sn/Cu layers that form whiskers/hillocks. To increase the efficiency of EBSD measurement, we developed a novel peel-off method to prepare Sn-Cu bi-layer samples with ultra-flat surfaces. This

enables most grains in the large area of interest to be indexed over repeated EBSD scans.

Studies were performed to determine why whiskers/hillocks initiate from specific sites on the surface. Correlation of the orientation maps with the surface morphology shows that the hillocks tend to start from (001) oriented grains surrounded by grains with (010) orientation. We emphasize that the hillock orientation changes significantly as the feature grows, so that the orientation of a whisker/hillock after growth is not necessarily the same as that of the grain from which it initiated. This points out the importance of tracking the surface evolution with time so that the surface deformation can be correlated with the initial grain structure.

Cross sections of the whisker/hillock indicated that most of them had oblique grain boundaries (v-grooves) under them. These presumably act as sinks where atoms can be incorporated into the growing grain while creating less stress than if they were columnar grains. Other measurements showed that surface defects, a weak oxide, dynamic recrystallization, or excessive IMC growth are not precursors for whiskers/hillocks to nucleate at particular surface sites. The grains that formed into whiskers/hillocks were present in the as-deposited samples, although this may not be universally true for other film preparation techniques, textures, or microstructures and needs to be studied.

As Sn is a highly anisotropic material, variation in the mechanical behavior or diffusivity of the grains in the polycrystalline Sn film may also explain why certain configurations are preferable for whisker/hillock formation. In the future, we will use the measured grain structure as an input to an FEA simulation to model the evolution of elastic stress and plastic deformation at different grains to determine the local stress and strain energy density.

### ACKNOWLEDGEMENTS

The authors gratefully acknowledge help from Allan Bower and Gordon Barr and the support from the NSF under contract DMR0856229 and the NSF-sponsored MRSEC (contract DMR0079964).

### REFERENCES

1. Multiple examples of whisker-induced failures are documented on the NASA website, <http://nepp.nasa.gov/whisker/>.
2. S.M. Arnold, *Plating* 53, 96 (1966).
3. J.Y. Tsai, Y.C. Hu, C.M. Tsai, and C.R. Kao, *JEM* 32, 1203 (2003).
4. C.M. Chuang and K.L. Lin, *JEM* 32, 1426 (2003).
5. J.Y. Park, R. Kabade, C.U. Kim, T. Carper, S. Dunford, and V. Puligandla, *JEM* 32, 1474 (2003).
6. W.J. Tomlinson and I. Collier, *J. Mater. Sci.* 22, 1835 (1987).
7. N. Jadhav, Brown University, Providence, RI, unpublished research, 2012.
8. B.Z. Lee and D.N. Lee, *Acta Mater.* 46, 3701 (1998).
9. K.N. Tu, *Phys. Rev. B* 49, 2030 (1994).
10. W.J. Boettinger, C.E. Johnson, L.A. Bendersky, K.W. Moon, M.E. Williams, and G.R. Stafford, *Acta Mater.* 53, 5033 (2005).

11. N. Jadhav, E.J. Buchovecky, L. Reinbold, S. Kumar, A.F. Bower, and E. Chason, *IEEE Trans. Electron. Packag. Manuf.* 33, 183 (2010).
12. E. Chason, N. Jadhav, W.L. Chan, L. Reinbold, and K.S. Kumar, *Appl. Phys. Lett.* 92, 171901 (2008).
13. E.J. Buchovecky, N.N. Du, and A.F. Bower, *Appl. Phys. Lett.* 94, 191904 (2009).
14. J.W. Shin and E. Chason, *J. Mater. Res.* 24, 1522 (2009).
15. M.W. Barsoum, E.N. Hoffman, R.D. Doherty, S. Gupta, and A. Zavaliangos, *Phys. Rev. Lett.* 93, 206104 (2004).
16. N. Jadhav, E. Buchovecky, E. Chason, and A. Bower, *JOM* 62, 30 (2010).
17. J. Smetana, *IEEE Trans. Electron. Packag. Manuf.* 30, 11 (2007).
18. P.T. Vianco and J.A. Rejent, *J. Electron. Mater.* 38, 1815 (2009).
19. G.L. Wynick and C.J. Boehlert, *Mater. Charact.* 55, 190 (2005).
20. F. Pei, Brown University, Providence, RI, unpublished research, 2011.
21. W.J. Choi, T.Y. Lee, K.N. Tu, N. Tamura, R.S. Celestre, A.A. MacDowell, Y.Y. Bong, and L. Nguyen, *Acta Mater.* 51, 6253 (2003).
22. M. Sobiech, M. Wohlschlägel, U. Welzel, E.J. Mittemeijer, W. Hugel, A. Seekamp, W. Liu, and G.E. Ice, *Appl. Phys. Lett.* 94, 221901 (2009).
23. A. Frye, G.T. Galyon, and L. Palmer, *IEEE Trans. Electron. Packag. Manuf.* 30, 2 (2007).
24. F. Pei, N. Jadhav, and E. Chason, *Appl. Phys. Lett.* 100, 221902 (2012).
25. W. Zhang, A. Egli, F. Schwager, and N. Brown, *IEEE Trans. Electron. Packag. Manuf.* 28, 85 (2005).
26. E. Buchovecky, N. Jadhav, A.F. Bower, and E. Chason, *J. Electron. Mater.* 38, 2676 (2009).
27. K.S. Kumar, L. Reinbold, A.F. Bower, and E. Chason, *J. Mater. Res.* 23, 2916 (2008).